

Polymer-stabilized Cas9 nanoparticles and modified repair templates increase genome editing efficiency

David N. Nguyen^{1,2,3,4,13}, Theodore L. Roth^{2,3,4,5,6,13}, P. Jonathan Li^{2,3,4}, Peixin Amy Chen^{2,3,4}, Ryan Apahty^{2,3,4}, Murad R. Mamedov^{2,3,4}, Linda T. Vo³, Victoria R. Tobin^{2,3,4}, Daniel Goodman^{2,3,4}, Eric Shifrut^{2,3,4}, Jeffrey A. Bluestone^{3,7}, Jennifer M. Puck⁸, Francis C. Szoka^{1,9} and Alexander Marson^{1,2,3,4,10,11,12*}

Versatile and precise genome modifications are needed to create a wider range of adoptive cellular therapies^{1–5}. Here we report two improvements that increase the efficiency of CRISPR-Cas9-based genome editing in clinically relevant primary cell types. Truncated Cas9 target sequences (tCTTs) added at the ends of the homology-directed repair (HDR) template interact with Cas9 ribonucleoproteins (RNPs) to shuttle the template to the nucleus, enhancing HDR efficiency approximately two- to fourfold. Furthermore, stabilizing Cas9 RNPs into nanoparticles with polyglutamic acid further improves editing efficiency by approximately twofold, reduces toxicity, and enables lyophilized storage without loss of activity. Combining the two improvements increases gene targeting efficiency even at reduced HDR template doses, yielding approximately two to six times as many viable edited cells across multiple genomic loci in diverse cell types, such as bulk (CD3⁺) T cells, CD8⁺ T cells, CD4⁺ T cells, regulatory T cells (Tregs), γδ T cells, B cells, natural killer cells, and primary and induced pluripotent stem cell-derived⁶ hematopoietic stem progenitor cells (HSPCs).

We recently reported an approach to reprogram human T cells with CRISPR-based genome targeting without the need for viral vectors⁵ by which we found that varying the relative concentrations of both Cas9 ribonucleoprotein (RNP) and homology-directed repair (HDR) template had significant effects on targeting efficiency and toxicity. However, many research and clinical applications still depend on improving efficiency, cell viability, and generalizability of non-viral genome targeting across cell types^{1–4}. Here, we set out to optimize the interactions between the HDR template and nanoparticle-stabilized RNPs to further improve genome editing efficiency independent of cell type.

We devised a novel approach to promote nuclear entry of the template. Unlike previous efforts that used complex covalent linkages⁷, we attempted to recruit Cas9 RNPs with nuclear localization sequences (NLSs) to the HDR template by enhancing Watson–Crick

interactions. CRISPR–Cas9 interacts specifically with both genomic and non-genomic double stranded DNA (dsDNA)⁸, and nuclease-deficient Cas9 (dCas9) has been used in many applications to localize protein and RNA effectors to specific DNA sequences without cleaving the target sequence⁹. We therefore tested whether we could enhance HDR by targeting a dCas9–NLS ‘shuttle’ to the ends of an HDR template by coding 20 bp Cas9 target sequences (CTTs) at the ends of the homology arms (Supplementary Fig. 1). Indeed, CTS-modified HDR templates mixed with dCas9–NLS RNP did show mild improvements in HDR efficiency in primary human T cells (Supplementary Fig. 1) but required two distinct RNPs (with dCas9 and catalytically active Cas9). These data led us to search for a simplified method that uses the same RNP to both cut a specified genomic site and recruit Cas9–NLS to HDR templates.

We reasoned that a single catalytically active Cas9–NLS RNP would suffice for both on-target genomic cutting and ‘shuttling’ if the HDR template were designed with 16 bp truncated CTTs (tCTTs) that enable Cas9 binding but do not enable cutting¹⁰ (Fig. 1a and Supplementary Fig. 2). With the proper sequence orientation, the addition of tCTTs markedly improved knock-in efficiency of a 1.5 kb DNA sequence inserting a reprogrammed TCRα and TCRβ specificity at the endogenous TRAC (T cell receptor α constant) locus (Fig. 1b and Supplementary Fig. 2). This tCTS shuttle system also improved genome targeting efficiencies across a variety of loci in different primary human T cell subsets (Fig. 1c,d and Supplementary Fig. 3). HDR templates with the tCTTs achieved preferential targeting even in direct competition with unmodified dsDNA HDR templates simultaneously delivered to the same cells (Fig. 1e and Supplementary Fig. 4). In addition, the tCTS shuttle improved efficiencies of bi-allelic and multiplexed targeting across different loci (Fig. 1f and Supplementary Fig. 4). The full HDR efficiency gains depended critically on the presence of an NLS in the Cas9 RNP, use of an on-target guide RNA (gRNA), and pre-incubation of the Cas9–NLS RNP with the tCTS-modified HDR template (Fig. 1g and Supplementary Fig. 5). Taken together, these

¹Department of Medicine, University of California, San Francisco, San Francisco, CA, USA. ²Department of Microbiology and Immunology, University of California, San Francisco, San Francisco, CA, USA. ³Diabetes Center, University of California, San Francisco, San Francisco, CA, USA. ⁴Innovative Genomics Institute, University of California, Berkeley, Berkeley, CA, USA. ⁵Medical Scientist Training Program, University of California, San Francisco, San Francisco, CA, USA. ⁶Biomedical Sciences Graduate Program, University of California, San Francisco, San Francisco, CA, USA. ⁷Sean N. Parker Autoimmune Research Laboratory, University of California, San Francisco, San Francisco, CA, USA. ⁸Division of Allergy, Immunology, and Bone Marrow Transplantation, Department of Pediatrics, University of California, San Francisco, San Francisco, CA, USA. ⁹Department of Bioengineering and Therapeutic Sciences, School of Pharmacy, University of California, San Francisco, San Francisco, CA, USA. ¹⁰Chan Zuckerberg Biohub, San Francisco, CA, USA. ¹¹UCSF Helen Diller Family Comprehensive Cancer Center, University of California, San Francisco, San Francisco, CA, USA. ¹²Parker Institute for Cancer Immunotherapy, San Francisco, CA, USA. ¹³These authors contributed equally: David N. Nguyen, Theodore L. Roth. *e-mail: alexander.marson@ucsf.edu

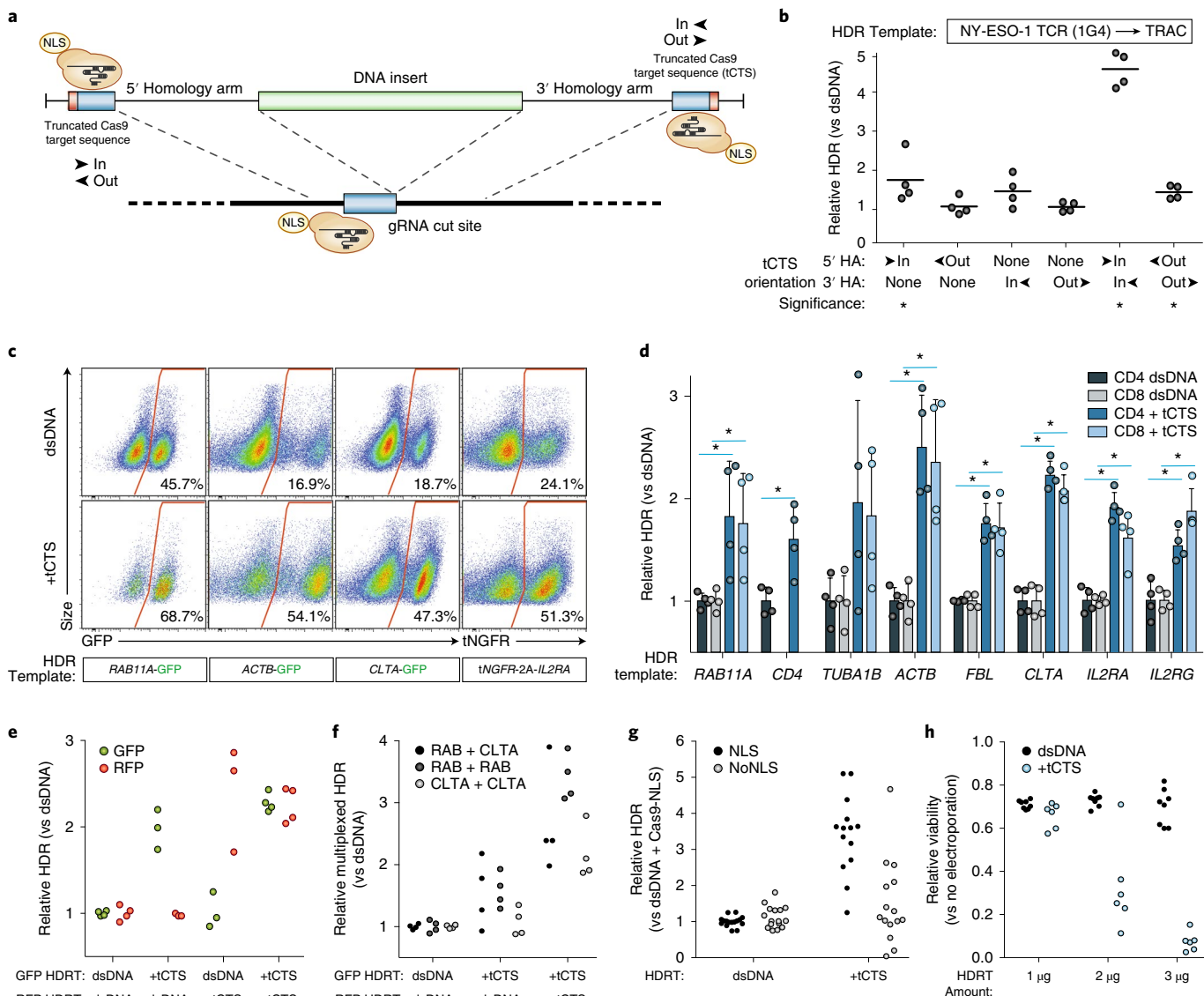


Fig. 1 | Truncated tCTSSs in HDR templates increase large non-viral knock-in efficiency. **a**, Enzymatically active Cas9-NLS RNPs can bind tCTSSs added to the ends of an HDR template (HDRT). **b**, ‘In’ facing orientation of the tCTSSs (protospacer adjacent motif (PAM) facing in towards the center of the inserted sequence versus ‘out’ away from the insert) on the edges of both the 5’ and 3’ homology arms improved knock-in efficiency of a new TCR α -TCR β specificity at the endogenous TRAC locus. *P < 0.05 (Mann-Whitney test vs no tCTS control). **c**, Representative flow cytometry plots showed improved targeting efficiency across target genomic loci with the tCTS modifications compared to an unmodified dsDNA HDR template. **d**, The tCTS modifications improved targeting efficiencies of large knock-ins across eight genomic loci tested in both CD4 $+$ and CD8 $+$ T cells. Note that CD4-GFP expression was not observed at relevant levels in CD8 $+$ T cells, as expected. *P < 0.05 (two-way paired t-test with Holm-Sidak multiple comparison correction). **e**, Multiplexed electroporation of GFP and RFP knock-in templates to the RAB11A locus where no, one, or both templates had a tCTS modification revealed direct competitive knock-in advantage of the ‘shuttle’ system compared to an unmodified dsDNA template (technical replicates from n = 2 donors). **f**, The tCTS modification improved multiplexed dual knock-in at different genomic loci as well as bi-allelic knock-in at a single target locus (technical replicates from n = 2 donors). **g**, Full improvement of knock-in efficiencies with the tCTS modifications (but not with unmodified dsDNA HDR templates) was dependent on the presence of an NLS on the Cas9 protein (multiple technical replicates from n = 2 donors). **h**, Decreased viability was seen with the tCTS modifications at lower DNA concentrations compared to unmodified dsDNA HDR template. The relative rates of HDR (**b,d,e,g**), multiplexed HDR (**f**), or viability (**h**) with the tCTS shuttle are displayed normalized to unmodified dsDNA HDR template (**b,d,e,g**) or to no electroporation controls (**h**) in n = 4 biologically independent blood donors (different healthy donors were used for some templates) (**b-d**) or from n = 2 biologically independent blood donors with multiple technical replicates shown to illustrate variance (**e-h**). Center lines indicate mean (**b,d**), error bars indicate standard deviation (**d**). HDR efficiency was measured 4 d after electroporation, and viability (total number of live cells relative to no electroporation control) was measured 2 d after electroporation.

data demonstrate that coupling an HDR template with tCTSSs to a Cas9–NLS RNP can enhance genome targeting efficiency without requiring modification of the protein or gRNA.

Exogenous DNA (including HDR templates) can be cytotoxic at high concentrations^{4,5,11}. We therefore assayed the effects of the

RNP–HDR template interactions on cell viability. Gene targeting using tCTS-modified HDR templates improved efficiency, but we observed decreased cell viability with tCTS-modified HDR templates at doses lower than unmodified dsDNA HDR templates (Fig. 1h). Decreased viability was only observed with an on-target

gRNA and pre-incubation of the RNP with tCTS-modified HDR template; it did not depend entirely on the presence of the NLS on Cas9 (Supplementary Fig. 5c), consistent with possible enhanced cytoplasmic delivery of DNA during electroporation due to the RNP–HDR template interaction.

In previous experiments, we observed that Cas9 RNP co-delivery could mitigate exogenous DNA toxicity (from unmodified plasmids or dsDNA templates) in human T cells⁵. We therefore wondered whether optimizing RNP delivery could improve effects on cell viability. We noted that the Cas9 protein itself appears to be only quasi-stable when complexed with gRNA; a molar excess of protein (RNA to Cas9 protein molar ratio of <1.0) results in a milky, opaque solution with rapid sedimentation (Fig. 2a) of poorly functional material (Supplementary Fig. 6a). Previous reports have suggested that RNP electroporation can be improved with addition of extra guide RNA or non-homologous single strand oligo (ssODNenh)¹². Excess gRNA or addition of ssODNenh dispersed the Cas9 RNPs (Supplementary Fig. 6b) and boosted editing efficiency of electroporated RNPs (Supplementary Fig. 6c). However, a combination of both gRNA and ssODNenh in excess did not further improve editing (Supplementary Fig. 6c), suggesting a possible shared mechanism of action.

We reasoned that the polymeric and anionic nature of nucleic acids shields excess positively charged residues of the Cas9 protein from nearby exposed portions of Cas9-bound gRNA, thus preventing aggregation and improving RNP particle stability. We therefore screened various commercially available water-soluble biological and synthetic polymeric materials for the ability to also enhance electroporation-mediated Cas9 knockout editing. Multiple different anionic polymers such as poly-L-glutamic acid (PGA), polyaspartic acid, heparin, and polyacrylic acid all enhanced editing efficiency in a dose-dependent manner without addition of ssODNenh or excess gRNA (Fig. 2b). The charge-neutral material polyethyleneglycol (PEG) had only minimal impact on RNP activity; the positively charged polymers polyethylenimine, protamine sulfate, poly-L-lysine, poly-L-ornithine, and poly-L-arginine all reduced editing efficiency (and viability) (Fig. 2b), thus establishing anionic charge as a key factor for RNP enhancement. Furthermore, enhancement

of RNP-based editing depended on polymer chain length (Supplementary Fig. 7), which is similar to the reported length dependence of ssODNenh¹² and consistent with colloid-stabilizing biomaterials¹³. Comparison of particle sizes by dynamic light scattering (DLS) revealed that Cas9 protein by itself was 10–15 nm in diameter, as expected for dispersed individual molecules, but that aggregates of approximately 200 nm size and larger were formed when gRNA was added (Fig. 2c and Supplementary Fig. 8). However, the addition of either PGA or ssODNenh prevented aggregation into micron-sized particles (Fig. 2d) and improved the size distribution of RNP nanoparticles to less than 100 nm on average, with peaks around 20 nm and in the 100–120 nm range (Fig. 2c and Supplementary Fig. 8).

We next tested whether anionic polymers could also enhance non-viral knock-in genome targeting. PGA was effective in enhancing knock-in editing in primary T cells (Fig. 2e) when it was mixed with Cas9 RNPs and a reduced concentration of an unmodified dsDNA template targeting integration of a *RAB11A*–GFP fusion. PGA-stabilized RNP nanoparticles promoted efficiency gains in primary human T cells (Fig. 2f) and appeared to reduce the toxicity of higher doses of HDR template (Fig. 2g). These efficiency gains were independent of the order of PGA addition, gRNA source, or Cas9 nuclease manufacturer (Supplementary Figs. 9–11). The combination of ssODNenh or higher gRNA concentrations with PGA did not further enhance knock-in efficiency, consistent with shared mechanisms due to the polymeric anionic charge of these molecules (Supplementary Fig. 12). This does not preclude contributions of additional material-specific properties, such as the stability of the PGA polymer during lyophilization. RNP stabilization with PGA (but not ssODNenh) permitted freeze–thaw cycles or lyophilization with retained knockout and knock-in editing activity (Fig. 2h and Supplementary Fig. 13). PGA-stabilized RNP nanoparticles therefore enhanced edited cell viability and could be stored dry, enabling significant streamlining of gene-modified cell manufacturing for research or clinical translation.

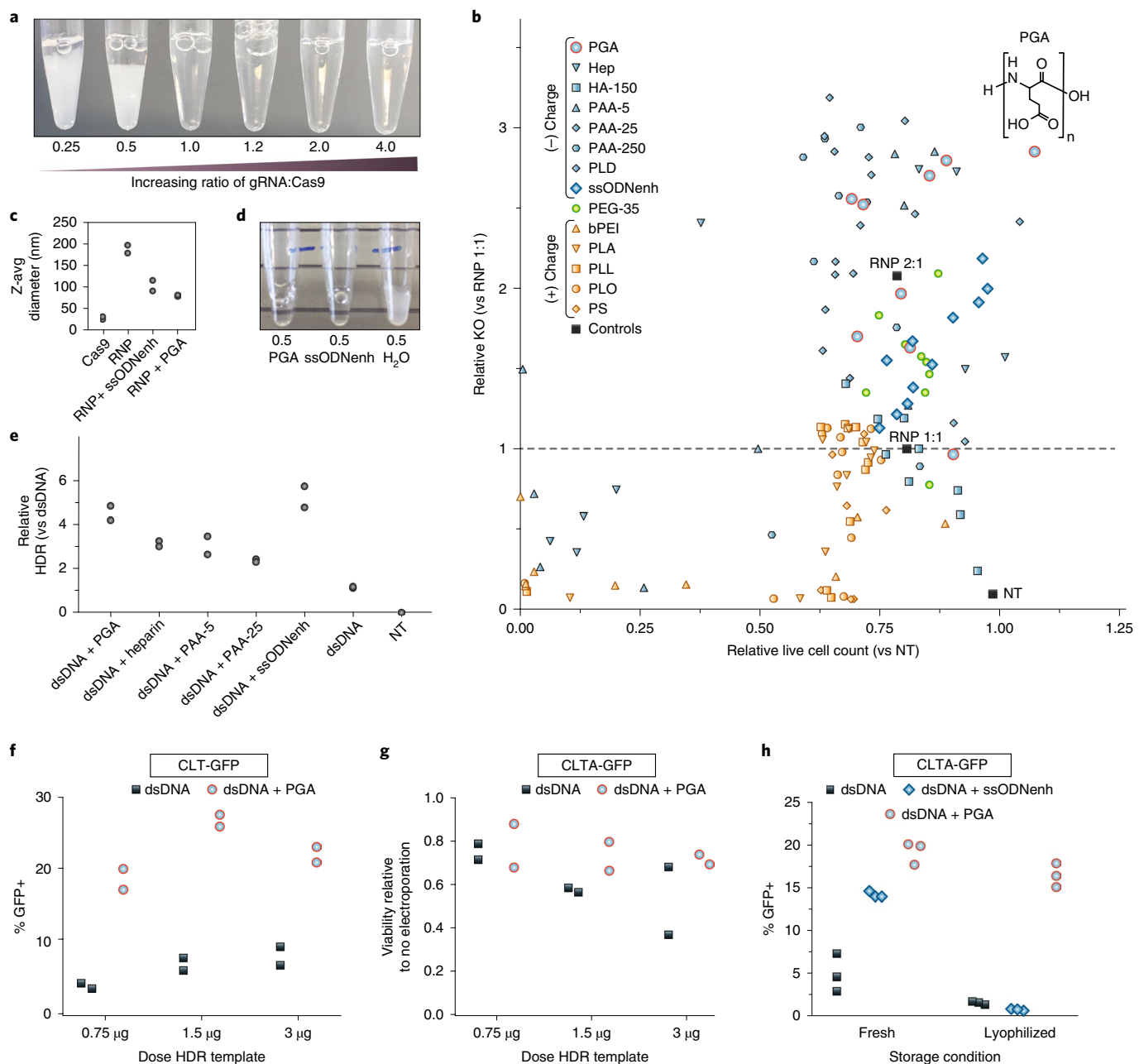
We further tested to ensure that combining the tCTS ‘shuttle’ and anionic polymers improved both the efficiency and resulting cell viability of non-viral genome targeting. Improved efficiency

Fig. 2 | Stabilizing Cas9 RNP nanoparticles with anionic polymers improves editing outcomes. **a**, Photograph taken 15 min after mixing gRNA and Cas9 protein incubated at 37 °C to form RNPs. Cas9 RNPs prepared at a low molar ratio of gRNA:protein appeared cloudy and rapidly settled out of solution. Representative photograph of $n=3$ independent experiments. **b**, Multiple polymers were screened for the ability to enhance *CD4* gene knockout editing when mixed with RNPs formulated at a 1:1 gRNA:protein ratio and electroporated into primary human CD4⁺ T cells. Loss of surface CD4 expression at 3 d assessed by flow cytometry is normalized to unenhanced editing efficiency (RNP 1:1 without any additive) on the y axis, and the live cell count is normalized to non-electroporated (NT) cells on the x axis. Negatively charged polymers are shown in blue: PGA; heparin sulfate (Hep); hyaluronic acid at 150 kDa (HA-150); polyacrylic acid at 5 kDa (PAA-5), 25 kDa (PAA-25), or 250 kDa (PAA-250); poly-L-aspartic acid (PLD), and ssODNenh. The neutral polymer PEG at 35 kDa (PEG-35) is shown in green, and positively charged polymers polyethylenimine at 25 kDa (PEI), poly-L-arginine at 15–70 kDa (PLA), poly-L-lysine 15–30 kDa (PLL), poly-L-ornithine at 30–70 kDa (PLO), and protamine sulfate (PS) are shown in orange. The chemical structure of PGA is shown as an inset above the data point that corresponds to 100 mg ml⁻¹ PGA. Each polymer sample was tested at serial dilutions to avoid the potential for dose-dependent cytotoxicity to falsely mask its impact on editing efficiency, and each concentration is depicted as an individual point that is an average of data from two different blood donors. **c**, PGA and ssODNenh stabilized and reduced the size of RNP nanoparticles. Cas9 RNPs prepared at a 2:1 molar ratio of gRNA:protein alone (RNP) or mixed with PGA or ssODNenh were assessed for hydrodynamic particle size by DLS. Z-average particle size is shown for $n=2$ independent preparations (individual sample size distributions and peaks are shown in Supplementary Fig. 8). **d**, Cas9 RNPs at 0.5 molar ratio of gRNA:protein (prepared as in **a**) could be further dispersed with addition of PGA or ssODNenh, whereas dilution with water alone had no visible benefit. Representative photograph of three repeated independent experiments. **e**, Multiple anionic polymers boosted knock-in editing efficiency. Polymers mixed with Cas9 RNPs prepared at a 2:1 gRNA:protein ratio were further mixed with 1 µg unmodified dsDNA HDR templates (targeting insertion of an amino-terminal fusion of GFP to *RAB11A*) and electroporated into CD4⁺ T cells; editing efficiency was assessed by flow cytometry at day 3. The relative rates of HDR are displayed compared to unmodified dsDNA HDR template without enhancer. Data are shown for each of $n=2$ biologically independent blood donors. **f,g**, PGA-stabilized Cas9 RNPs prepared at a 2:1 gRNA:protein ratio markedly improved knock-in editing in primary human bulk (CD3⁺) T cells targeting a carboxy-terminal fusion of GFP to clathrin (**f**) and improved the viability of electroporated cells compared to untreated cells (**g**). Data are shown for each of $n=2$ biologically independent blood donors. **h**, Cas9 RNPs prepared at a 2:1 gRNA:protein ratio with or without PGA or ssODNenh were mixed with 1 µg of unmodified dsDNA HDR template targeting an N-terminal fusion of GFP to *RAB11A*, lyophilized overnight, stored dry at -80 °C, and later reconstituted in water prior to electroporating into primary human bulk (CD3⁺) T cells. PGA-stabilized Cas9 nanoparticles were protected through lyophilization and reconstitution and retained activity for robust knock-in editing. Three technical replicates are shown for $n=1$ blood donor, representative of two independent experiments.

and cell recovery were consistent across human blood donors when the endogenous TCR was replaced with a therapeutically relevant TCR that recognizes the NY-ESO-1 tumor antigen (Supplementary Fig. 14). An increased dose of HDR template with or without the tCTS modification could improve the fraction of knock-in edited cells (Supplementary Fig. 14a,c), and the dose-dependent toxicity observed with the tCTS-modified HDR template (Fig. 1h) was mitigated by PGA-stabilized RNPs (Supplementary Fig. 14b,d). The maximal knock-in cell yield was achieved with a combination of PGA-stabilized RNPs and a reduced dose of tCTS-modified HDR templates (Supplementary Fig. 14). Importantly, the tCTS-modified HDR templates with PGA-stabilized RNPs markedly enhanced both knock-in efficiency and viability (Fig. 3a), and improved the recovery of viable T cells edited at a variety of endogenous genomic loci (Fig. 3b).

We also assessed the potential for off-target genome editing events, given concern that improved delivery of RNPs via stabilization into nanoparticles could increase both on- and off-target

double-strand breaks. With PGA, we observed only slightly increased off-target indel formation relative to RNP alone at previously identified off-target sites for the well-characterized gRNA targeting *EMX1* (refs. 14,15) as measured by deep amplicon sequencing¹⁶ (Supplementary Fig. 15a). We also investigated whether increased HDR template delivery via tCTS modifications would increase off-target transgene integration. As we have described previously, linear dsDNA templates can integrate and express transgenes through non-homology-directed mechanisms modeled by introducing a targeted cut at an off-target site⁵. Using this functional test for off-target integrations, we found that the addition of tCTSs for off-target guides or scrambled guides did not increase off-target expression of a GFP transgene compared to standard dsDNA HDR templates (Supplementary Fig. 15b,c). Although further work will be needed to assess the global off-target edits and integrations for specific RNPs and HDR templates, these results suggest that PGA and modified templates can boost knock-in targeting markedly while minimizing increases in undesirable outcomes.



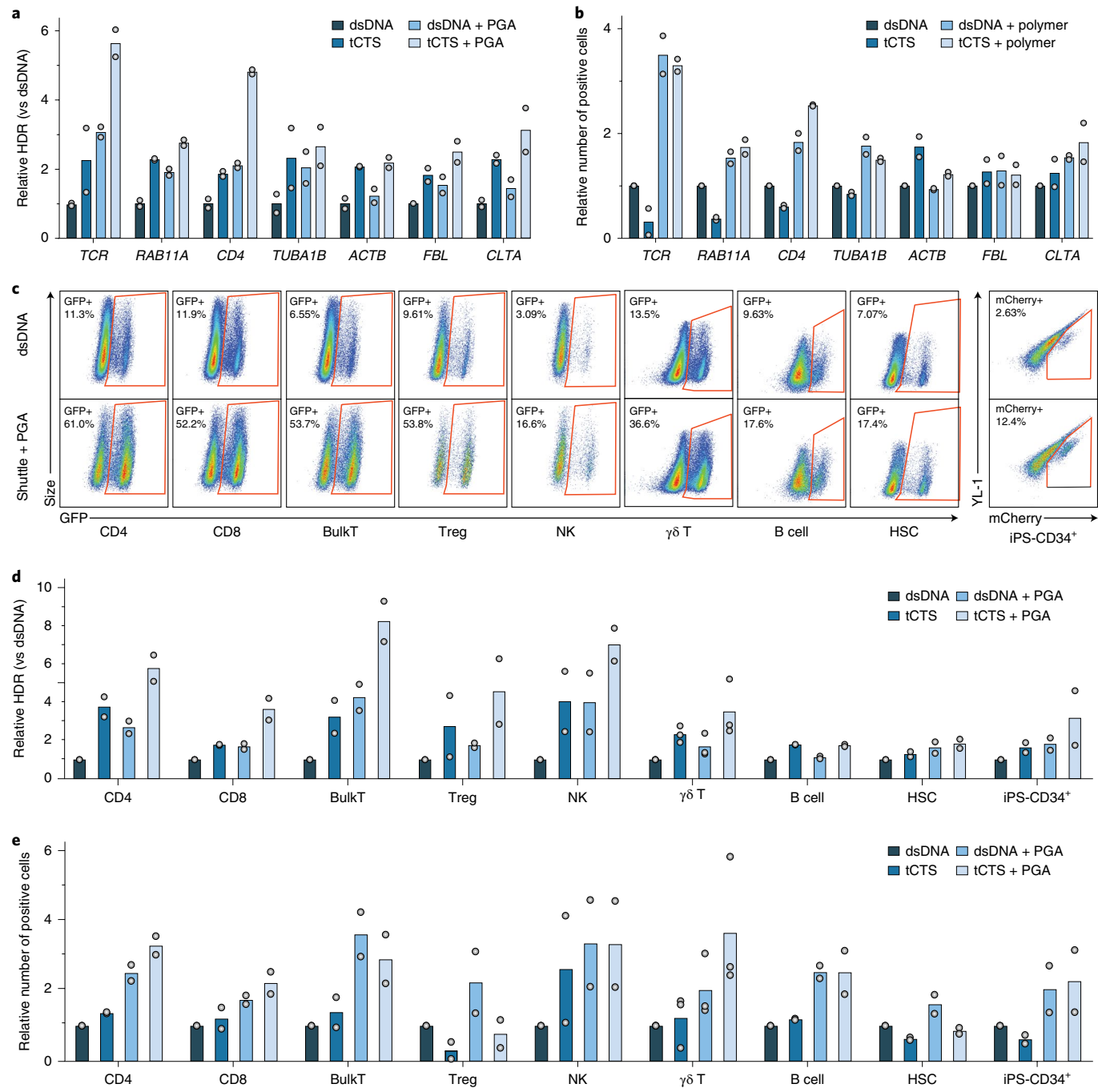


Fig. 3 | PGA-stabilized Cas9 RNP and tCTS-modified HDR templates improved knock-in gene editing outcomes across a variety of genetic loci and clinically relevant immune cell types. **a,b**, Cas9 RNPs were prepared at a 2:1 gRNA:protein ratio with or without PGA polymer and mixed with high doses (2–4 μ g) of regular dsDNA or tCTS-modified HDR template targeting knock-in at multiple genomic loci: transgenic NY-ESO 1 tumor antigen TCR into the TRAC locus, or GFP fusion at the N-terminus or C terminus of RAB11A, CD4, TUBA1B, ACTB, FBL or CLTA genes. The combination of PGA-stabilized Cas9 RNP nanoparticles and ‘shuttle’ tCTS-modified HDR template improved relative frequency of HDR (**a**) and resulted in a higher yield of successfully edited cells (**b**). **c–e**, Cas9 RNPs were prepared at a 2:1 gRNA:protein ratio with or without PGA polymer and mixed with low doses (0.5–1 μ g) of unmodified dsDNA or ‘shuttle’ tCTS-modified HDR templates targeting knock-in of GFP or mCherry to the N terminus of clathrin. The PGA-stabilized Cas9 RNP nanoparticles and tCTS-modified HDR templates improved editing efficiency in a variety of primary human immune cell types, as visualized in representative flow cytometry plots (after gating for live cells and respective cell-type-specific surface markers) (**c**) or expressed as relative frequency of GFP or mCherry positive cells (**d**), and resulted in a higher yield of successfully edited cells (**e**). The relative rates of HDR (**a,d**) and edited cell recovery (**b,e**) are displayed normalized to unmodified dsDNA HDR template without enhancer for each gene locus (**a,b**) or cell type (**d,e**). Data are shown for each of $n=2$ (for CD4, CD8, bulk (CD34⁺) T cells (BulkT), Tregs, NK cells, B cells, or HSCs) or $n=3$ (for $\gamma\delta$ T cells) biologically independent blood donor, or $n=2$ independently derived cell lines (iPS-CD34⁺). Data in (**c**) are representative of two repeated independent experiments.

Led by these results in T cells, we applied the combined system to enable non-viral genome targeting in a wider set of therapeutically relevant primary human hematopoietic cells. Using a tem-

plate encoding a GFP fusion to the vesicle-coating protein clathrin (encoded by the CLTA gene), which should be broadly expressed across many cell types, we consistently observed improved

editing efficiencies with the combined system (Fig. 3c–e). Bulk CD3⁺ T cells, purified CD4⁺ T cells or CD8⁺ T cells, and purified CD127^{low}CD25⁺CD4⁺ regulatory T cells (Tregs) all achieved a similarly high knock-in efficiency of up to >50% of cells, with a three- to eightfold increase in the percentage of knock-in edited cells at reduced HDR template concentrations (Fig. 3c,d). Although standard RNP and unmodified HDR templates achieved only minimal knock-in in isolated primary human natural killer (NK) cells or B cells, the combined system resulted in over 15% transgene-positive cells and an approximately two- to fivefold increase in edited cell yield (Fig. 3c–e). In γδ T cells, the combined system exhibited improved editing efficiency from approximately 5% to approximately 28% and a five- to sixfold improvement in edited cell recovery compared with a standard RNP and unmodified HDR template. Finally, we were able to express large transgene insertions in over 15% of human CD34⁺ hematopoietic stem progenitor cells (HSPCs) without a viral vector in both primary mobilized peripheral blood- and induced pluripotent stem cell (iPS)-derived⁶ CD34⁺ HSPCs, with approximately two- to threefold increases in yield of knock-in edited cells. The combined non-viral system was thus effective in diverse human hematopoietic cell types.

Together, PGA as an RNP nanoparticle-stabilizing enhancer and the tCTS-modified HDR template enabled high percentage editing with improved edited cell yields in a variety of primary hematopoietic cell types, opening the door to next-generation adoptive cell therapies beyond T cells. The combined nanoparticle-tCTS template system is a novel platform for exploring gene function in clinically relevant cell types whose genomes have previously been challenging to modify. The formation of PGA-stabilized RNP nanoparticles and the use of PCR primers to introduce tCTS modifications to HDR templates are both methods that can be adapted rapidly to any existing Cas9 RNP-based editing protocol. Notably, marked improvements in large gene targeting to endogenous loci were achieved without further optimizing cell cycle dynamics, small molecule modulation of DNA repair machinery, or specialized chemistries; these complementary strategies may eventually offer additional efficiency gains. Some variation in targeting success remains, depending on locus, knock-in sequence, electroporation parameters, and cell type. Further optimization of polymers or tCTS ‘shuttle’ configurations could offer additional improvements. Our data demonstrate a technically simple system that greatly enhances the capabilities of Cas9 RNP-mediated non-viral genome targeting in primary human hematopoietic cells and has direct translational potential for research, biotechnology, and clinical endeavors.

Online content

Any methods, additional references, Nature Research reporting summaries, source data, extended data, supplementary information, acknowledgements, peer review information; details of author contributions and competing interests; and statements of data and code availability are available at <https://doi.org/10.1038/s41587-019-0325-6>.

Received: 16 April 2019; Accepted: 25 October 2019;

Published online: 9 December 2019

References

- Yin, H., Xue, W. & Anderson, D. G. CRISPR-Cas: a tool for cancer research and therapeutics. *Nat. Rev. Clin. Oncol.* **16**, 281–295 (2019).
- Dunbar, C. E. et al. Gene therapy comes of age. *Science* **359**, eaan4672 (2018).
- Cornu, T. I., Mussolini, C. & Cathomen, T. Refining strategies to translate genome editing to the clinic. *Nat. Med.* **23**, 415–423 (2017).
- David, R. M. & Doherty, A. T. Viral vectors: the road to reducing genotoxicity. *Toxicol. Sci.* **155**, 315–325 (2017).
- Roth, T. L. et al. Reprogramming human T cell function and specificity with non-viral genome targeting. *Nature* **559**, 405–409 (2018).
- Vo, L. T. et al. Regulation of embryonic haematopoietic multipotency by EZH1. *Nature* **553**, 506–510 (2018).
- Pouton, C. W., Wagstaff, K. M., Roth, D. M., Moseley, G. W. & Jans, D. A. Targeted delivery to the nucleus. *Adv. Drug Deliv. Rev.* **59**, 698–717 (2007).
- Doudna, J. A. & Charpentier, E. Genome editing. The new frontier of genome engineering with CRISPR-Cas9. *Science* **346**, 1258096 (2014).
- Dominguez, A. A., Lim, W. A. & Qi, L. S. Beyond editing: repurposing CRISPR-Cas9 for precision genome regulation and interrogation. *Nat. Rev. Mol. Cell Biol.* **17**, 5–15 (2016).
- Jiang, F. & Doudna, J. A. CRISPR-Cas9 Structures and Mechanisms. *Annu. Rev. Biophys.* **46**, 505–529 (2017).
- Luecke, S. et al. cGAS is activated by DNA in a length-dependent manner. *EMBO Rep.* **18**, 1707–1715 (2017).
- Richardson, C. D., Ray, G. J., Bray, N. L. & Corn, J. E. Non-homologous DNA increases gene disruption efficiency by altering DNA repair outcomes. *Nat. Commun.* **7**, 12463 (2016).
- Bernkop-Schnurch, A. Strategies to overcome the polycation dilemma in drug delivery. *Adv. Drug Deliv. Rev.* **136-137**, 62–72 (2018).
- Vakulskas, C. A. et al. A high-fidelity Cas9 mutant delivered as a ribonucleoprotein complex enables efficient gene editing in human hematopoietic stem and progenitor cells. *Nat. Med.* **24**, 1216–1224 (2018).
- Tsai, S. Q. et al. CIRCLE-seq: a highly sensitive in vitro screen for genome-wide CRISPR-Cas9 nuclease off-targets. *Nat. Methods* **14**, 607–614 (2017).
- Clement, K. et al. CRISPResso2 provides accurate and rapid genome editing sequence analysis. *Nat. Biotechnol.* **37**, 224–226 (2019).

Publisher's note Springer Nature remains neutral with regard to jurisdictional claims in published maps and institutional affiliations.

© The Author(s), under exclusive licence to Springer Nature America, Inc. 2019

Methods

Cell culture. Primary adult cells were obtained from healthy human donors from leukoreduction chamber residuals after Trima Accel apheresis (Vitalant, formerly Blood Centers of the Pacific) or from freshly drawn whole blood under a protocol approved by the University of California San Francisco Institutional Review Board (IRB) or Vitalant IRB. Peripheral blood mononuclear cells were isolated by Ficoll-Paque (GE Healthcare) centrifugation using SepMate tubes (STEMCELL, as per the manufacturer's instructions). Specific lymphocytes were then further isolated by magnetic negative selection using an EasySep Human B Cell, CD4⁺ T Cell, bulk (CD3⁺) T Cell, CD8⁺ T cell, CD4⁺CD127^{low}CD25⁺ Regulatory T Cell, Gamma/Delta T Cell, or NK Cell Isolation kit (STEMCELL, as per the manufacturer's instructions).

Isolated CD4⁺, CD8⁺, bulk (CD3⁺) T cells, regulatory T cells (CD4⁺ CD127^{low} CD25⁺), or γδ T cells were activated and cultured for 2 d at 0.5 to 1.0 million cells ml⁻¹ in XVivo15 medium (Lonza) with 5% fetal bovine serum, 50 μM 2-mercaptoethanol, 10 mM N-acetyl L-cysteine, anti-human CD3/CD28 magnetic Dynabeads (Thermo Fisher) at a bead to cell ratio of 1:1, and a cytokine cocktail of IL-2 at 300 U ml⁻¹ (UCSF Pharmacy), IL-7 at 5 ng ml⁻¹ (R&D Systems), and IL-15 at 5 ng ml⁻¹ (R&D Systems). Activated T cells were collected from their culture vessels, and Dynabeads were removed by placing cells on an EasySep cell separation magnet (STEMCELL) for 5 min. Isolated B cells were cultured in IMDM (Thermo Fisher) with 5% fetal bovine serum, 100 ng ml⁻¹ MEGACD40L (Enzo), 1,000 ng ml⁻¹ CpG (InvivoGen), 500 U ml⁻¹ IL-2 (UCSF Pharmacy), 50 ng ml⁻¹ IL-10 (Thermo Fisher), and 10 ng ml⁻¹ IL-15 (R&D Systems). Freshly isolated NK cells were cultured in X-VIVO 15 medium (Lonza) with 5% fetal bovine serum, 50 μM 2-mercaptoethanol, and 10 mM N-acetyl L-cysteine, together with IL-2 (at 1,000 U ml⁻¹) and MACSbead Particles pre-loaded with anti-human CD335 (NKP46) and anti-human CD2 antibodies (Miltenyi Biotech). Primary adult peripheral blood G-CSF-mobilized CD34⁺ hematopoietic stem cells were purchased from StemExpress and cultured at 0.5 × 10⁶ cells ml⁻¹ in SFEM II medium supplemented with CC110 cytokine cocktail (STEMCELL) for 2 d prior to electroporation. Induced pluripotent stem (iPS) cells were generated and differentiated into CD34⁺ HSPCs as described previously⁶; then cultured in SFEM medium (STEMCELL) supplemented with IL-3 at 10 ng ml⁻¹, IL-6 at 50 ng ml⁻¹, SCF at 50 ng ml⁻¹, FLT-3L at 50 ng ml⁻¹, and TPO at 50 ng ml⁻¹ (PeproTech) and doxycycline at 2 μg ml⁻¹ (Sigma).

RNP formulation with polymers. Cas9 RNPs were formulated immediately prior to electroporation, except when frozen or lyophilized as described below. Synthetic CRISPR RNA (crRNA, with guide sequences listed in Supplementary Table 1) and trans-activating crRNA (tracrRNA) were chemically synthesized (Edit-R, Dharmacacon Horizon or Integrated DNA Technologies (IDT)), resuspended in 10 mM Tris-HCl (pH 7.4) with 150 mM KCl or IDT duplex buffer at a concentration of 160 μM, and stored in aliquots at -80°C. To make gRNA, aliquots of crRNA and tracrRNA were thawed, mixed 1:1 v/v, and annealed by incubation at 37°C for 30 min to form an 80 μM gRNA solution. For comparison, chemically modified gRNA was purchased from Synthego and resuspended according to the manufacturer's protocol. Cas9-NLS, dCas9-NLS, D10a Cas9-NLS¹⁷, and Cas9 without NLS were purchased from the University of California Berkeley QB3 MacroLab; HiFi Cas9 was purchased from IDT. To make RNPs, gRNA was further diluted in buffer first or directly mixed 1:1 v/v with 40 μM Cas9-NLS protein to achieve the desired molar ratio of gRNA:Cas9 (2:1 unless otherwise stated). Unless otherwise stated, the final dose of RNP per nucleofection was 50 pmol on a Cas9 protein basis.

For initial screening, polymers were purchased dry (see Supplementary Table 2) and resuspended to 100 mg ml⁻¹ in water (except as noted), passed through a 0.2 μm syringe filter, and stored at -80°C prior to use. The ssODNenh electroporation enhancer (with sequence listed in Supplementary Table 2) was synthesized (IDT) and resuspended to 100 μM in water. Serial dilutions of polymers or ssODNenh were made in water, then mixed 1:1 v/v with preformed RNPs. For subsequent knock-in experiments, 15–50 kDa PGA (Sigma) was resuspended to 100 mg ml⁻¹ in water, sterile filtered, and mixed with freshly prepared gRNA at a 0.8:1 volume ratio prior to complexing with Cas9 protein for a final volume ratio of gRNA:PGA:Cas9 of 1:0.8:1. RNP particle size was measured by DLS dispersed in PBS on a Zetasizer Nano ZS (Malvern Panalytical).

For RNP lyophilization, freshly prepared RNPs premixed with PGA or ssODNenh and HDR templates were diluted 1:1 v/v in 50 mM trehalose, flash frozen in a liquid nitrogen bath, immediately dried on a Labconco Freeze Dry System FreeZone 4.5 lyophilizer for 24 h, and stored at -20°C until use. Dry RNP was resuspended in water to achieve the original concentration, incubated for 5 min at 37°C, then mixed with cells for electroporation.

HDR template generation and electroporation. Long double-strand HDR templates encoding various gene insertions (see Supplementary Table 1) and 300–350 bp homology arms were synthesized as gBlocks (IDT) and cloned into a pUC19 plasmid, which then served as a template for generating a PCR amplicon. Specific PCR primers targeting the left and right homology arms with additional CTSs (see Supplementary Fig. 2) were synthesized (IDT) without chemical modifications.

Amplicons were generated as described previously⁵ with KAPA HiFi polymerase (Kapa Biosystems), purified by SPRI bead cleanup, and resuspended in water to 0.5–2 μg μl⁻¹ measured by light absorbance on a NanoDrop spectrophotometer (Thermo Fisher).

HDR templates were mixed and incubated with RNPs for at least 5 min prior to mixing with and electroporating into cells. Immediately prior to electroporation in a 96-well format 4D-Nucleofector (Lonza), cells were centrifuged for 10 min at 90 g, medium was aspirated, and cells were resuspended in the electroporation buffer P3 (Lonza) using 17–20 μl buffer per 0.5–1.0 × 10⁶ cells. T cells, NK cells, and B cells were electroporated with pulse code EH-115, primary HSPCs with pulse code ER-100, and iPS-derived CD34 HSPCs with pulse code EY-100. Immediately after electroporation, cells were rescued with the addition of 80 μL of growth medium directly into the electroporation well, incubated for 10–20 min, then removed and diluted to 0.5–1.0 × 10⁶ cells ml⁻¹ in growth medium. Additional fresh growth medium and cytokines were added every 48 h.

At 3–5 d after electroporation (except for NK cells collected at 5–7 d), cells were collected for staining and flow cytometry analysis. In brief, cells were stained for cell type-specific surface markers and live-dead discrimination (see list of antibodies in Supplementary Table 3), then analyzed on an Attune NxT flow cytometer with an automated 96-well sampler (Thermo Fisher) sampling a defined volume (50–150 μL per well) to obtain quantitative cell counts. Cytometry data were processed and analyzed using FlowJo software (BD Biosciences).

Amplicon sequencing for off-target editing. CD3⁺ (bulk) T cells were electroporated with various RNPs incorporating an EMX1 gRNA previously shown to have high levels of off-target cutting by CIRCLE-Seq⁵. Three days after editing, genomic DNA was extracted and purified with a Zymo Quick-DNA Miniprep kit. After normalizing input quantities of genomic DNA, a two-step PCR amplicon sequencing procedure was performed using NEB Q5 Hot Start 2X Master Mix polymerase with the manufacturer's recommended thermocycler conditions. An initial 18-cycle PCR reaction using previously validated primers¹⁴ (see Supplementary Table 1) was performed to an approximately 150–250 bp region centered on the predicted gRNA cut sites. After a 1.0× SPRI purification step, a second 14-cycle PCR was performed to append P5 and P7 Illumina sequencing adaptors and sample-specific barcodes, followed by another 1.0× SPRI purification. Concentrations were normalized across samples and pooled, and the amplicon library was sequenced on an Illumina MiniSeq with paired 300-base read run mode. Amplicon sequence reads were processed with the CRISPResso2 algorithm in batch mode¹⁶ using default parameters. We eliminated reads with potential sequencing errors detected as single base substitutions but no indels. The remaining reads identified as indels were used to calculate the non-homologous end joining (NHEJ) percentage at each on- or off-target site. We excluded two off-target sites where amplicon sequencing was performed but control-treated cells from both donors contained sequence variants at >5% of reads that were attributable to germline variants and/or PCR and sequencing errors at poly A/T sequences.

Statistical analysis. Unless otherwise stated in the figure legends, all experiments were repeated at least twice with biologically independent samples, and data were aggregated for display and analysis. For Fig. 1b, a two-way Mann-Whitney test was used to compare tCTS orientation and modifications to the control unmodified template, with $n=4$ biologically independent blood donors. For Fig. 1d, a two-way paired *t*-test with Holm-Sidak multiple comparison correction was used to compare relative HDR at each locus. Exact *P* values are available in Supplementary Table 4.

Reporting Summary. Further information on research design is available in the Nature Research Reporting Summary linked to this article.

Data availability

Amplicon sequencing data have been deposited in the National Institutes of Health NCBI SRA (Bioproject PRJNA564604), and flow cytometry raw data files are available upon request. Plasmids containing the HDR template sequences used in the study are available through AddGene (Supplementary Table 1), and annotated DNA sequences for all constructs are available upon request.

References

17. Ran, F. A. et al. Double nicking by RNA-guided CRISPR Cas9 for enhanced genome editing specificity. *Cell* **154**, 1380–1389 (2013).

Acknowledgements

We thank members of the Marson laboratory, C. Jeans and the QB3 MacroLab, and A. Dolor for suggestions and technical assistance. This research was supported by NIH grants DP3DK111914-01, R01DK119979, and P50GM082250 (A.M.), a grant from the Keck Foundation (A.M.), gifts from Jake Aronov, Barbara Bakar, and the American Endowment Foundation (A.M.), a gift from the UCSF Diabetes Center, a gift from the Jeffrey Modell Foundation, and a National Multiple Sclerosis Society grant

(A.M., CA 1074-A-21). D.N.N. was supported by the UCSF Biology of Infectious Diseases Training Program (T32A1007641), an NIH Loan Repayment Program grant (L40 AI140341), and the CIS CSL Behring Fellowship Award. T.L.R. was supported by the UCSF Medical Scientist Training Program (T32GM007618), the UCSF Endocrinology Training Grant (T32 DK007418), and the National Institute of Diabetes and Digestive and Kidney Disorders (F30DK120213). L.T.V. is supported by a Damon Runyon Postdoctoral Research Fellowship. A.M. holds a Career Award for Medical Scientists from the Burroughs Wellcome Fund, is an investigator at the Chan Zuckerberg Biohub, and has received funding from the Innovative Genomics Institute (IGI) and the Parker Institute for Cancer Immunotherapy. The UCSF Flow Cytometry Core was supported by the Diabetes Research Center grant NIH P30 DK063720.

Author contributions

D.N.N., T.L.R., and A.M. designed the study. T.L.R. conceived the template 'shuttle' system and performed all 'shuttle' optimization. D.G. suggested the use of truncated Cas9 target sequences. D.N.N. conceived the polymer stabilization of RNP system and performed all polymer optimizations. D.N.N., T.L.R., P.J.L., P.A.C., R.A., M.R.M., L.T.V., V.R.T., D.G., E.S., J.A.B., J.M.P., and F.C.S. contributed to the design and completion of

experiments combining the shuttle and polymer systems in additional primary cell types. D.N.N., T.L.R., and A.M. wrote the manuscript with input from all authors.

Competing interests

A.M. is a co-founder of Spotlight Therapeutics. T.L.R. and A.M. are co-founders of ArsenalBio. J.A.B. is a founder of Sonoma Biotherapeutics. A.M. serves on the scientific advisory board of PACT Pharma, is an advisor to Trizell, and was a former advisor to Juno Therapeutics. The Marson laboratory has received sponsored research support from Juno Therapeutics, Epinomics, and Sanofi, as well as a gift from Gilead. Patents have been filed based on the findings described here. All other authors have no competing interests.

Additional information

Supplementary information is available for this paper at <https://doi.org/10.1038/s41587-019-0325-6>.

Correspondence and requests for materials should be addressed to A.M.

Reprints and permissions information is available at www.nature.com/reprints.

Corresponding author(s): Alexander Marson

Last updated by author(s): Sep 27, 2019

Reporting Summary

Nature Research wishes to improve the reproducibility of the work that we publish. This form provides structure for consistency and transparency in reporting. For further information on Nature Research policies, see [Authors & Referees](#) and the [Editorial Policy Checklist](#).

Statistics

For all statistical analyses, confirm that the following items are present in the figure legend, table legend, main text, or Methods section.

n/a Confirmed

- The exact sample size (n) for each experimental group/condition, given as a discrete number and unit of measurement
- A statement on whether measurements were taken from distinct samples or whether the same sample was measured repeatedly
- The statistical test(s) used AND whether they are one- or two-sided
Only common tests should be described solely by name; describe more complex techniques in the Methods section.
- A description of all covariates tested
- A description of any assumptions or corrections, such as tests of normality and adjustment for multiple comparisons
- A full description of the statistical parameters including central tendency (e.g. means) or other basic estimates (e.g. regression coefficient) AND variation (e.g. standard deviation) or associated estimates of uncertainty (e.g. confidence intervals)
- For null hypothesis testing, the test statistic (e.g. F , t , r) with confidence intervals, effect sizes, degrees of freedom and P value noted
Give P values as exact values whenever suitable.
- For Bayesian analysis, information on the choice of priors and Markov chain Monte Carlo settings
- For hierarchical and complex designs, identification of the appropriate level for tests and full reporting of outcomes
- Estimates of effect sizes (e.g. Cohen's d , Pearson's r), indicating how they were calculated

Our web collection on [statistics for biologists](#) contains articles on many of the points above.

Software and code

Policy information about [availability of computer code](#)

Data collection

Provide a description of all commercial, open source and custom code used to collect the data in this study, specifying the version used OR state that no software was used.

Data analysis

Flow cytometric data was analyzed using FlowJo v.10. Graphs were created and statistics calculated using Graph Pad Prism v.8. Next gen sequencing of amplicons was analyzed by the CRISPresso2 algorithm.

For manuscripts utilizing custom algorithms or software that are central to the research but not yet described in published literature, software must be made available to editors/reviewers. We strongly encourage code deposition in a community repository (e.g. GitHub). See the Nature Research [guidelines for submitting code & software](#) for further information.

Data

Policy information about [availability of data](#)

All manuscripts must include a [data availability statement](#). This statement should provide the following information, where applicable:

- Accession codes, unique identifiers, or web links for publicly available datasets
- A list of figures that have associated raw data
- A description of any restrictions on data availability

Amplicon sequencing data has been deposited in the NIH NCBI SRA (Bioproject PRJNA564604) and flow cytometry raw data files are available upon request. Plasmids containing the HDR template sequences used in the study are available through AddGene (Supplementary Table 1), and annotated DNA sequences for all constructs are available upon request.

Field-specific reporting

Please select the one below that is the best fit for your research. If you are not sure, read the appropriate sections before making your selection.

Life sciences

Behavioural & social sciences

Ecological, evolutionary & environmental sciences

For a reference copy of the document with all sections, see nature.com/documents/nr-reporting-summary-flat.pdf

Life sciences study design

All studies must disclose on these points even when the disclosure is negative.

Sample size	Primary cells were obtained from at least two different healthy blood donors or more, subject to availability of blood donors for simultaneous measurements. Repeated experiments with additional unrelated healthy blood donors are pooled. For iPSC-CD34+ experiments, two independently-derived cell lines were available (Fig 3c-e). No power analyses were performed prior to experiments.
Data exclusions	Data were excluded if controls did not perform as expected. We excluded two off-target sites where amplicon sequencing was performed but control-treated cells from both donors contained sequence variants at >5% of reads that was attributable either to germline variants and/or PCR and sequencing errors at poly A/T sequences.
Replication	For all editing experiments findings were replicated in at least two independent healthy human donors.
Randomization	For all cell experiments, healthy blood donors were anonymous. No further randomization was undertaken.
Blinding	For all cell experiments, healthy blood donors were anonymous. No further blinding was undertaken.

Reporting for specific materials, systems and methods

We require information from authors about some types of materials, experimental systems and methods used in many studies. Here, indicate whether each material, system or method listed is relevant to your study. If you are not sure if a list item applies to your research, read the appropriate section before selecting a response.

Materials & experimental systems

- | | |
|-------------------------------------|-----------------------------|
| n/a | Involved in the study |
| <input type="checkbox"/> | Antibodies |
| <input checked="" type="checkbox"/> | Eukaryotic cell lines |
| <input type="checkbox"/> | Palaeontology |
| <input type="checkbox"/> | Animals and other organisms |
| <input checked="" type="checkbox"/> | Human research participants |
| <input type="checkbox"/> | Clinical data |

Methods

- | | |
|-------------------------------------|------------------------|
| n/a | Involved in the study |
| <input type="checkbox"/> | ChIP-seq |
| <input checked="" type="checkbox"/> | Flow cytometry |
| <input type="checkbox"/> | MRI-based neuroimaging |

Antibodies

Antibodies used

- Fc Receptor - Biolegend Human TruStain FcX 422302 @1:25
- GhostDye Red 780 - Tonbo - 13-0865-T500 @1:1000
- GhostDye Violet 510 - Tonbo - 13-0870-T500 @1:1000
- LIVE/DEAD® Fixable Aqua Dead Cell Stain - ThermoFisher Scientific - L34966 @1:1000
- CD19 PacBlue Biolegend HIB19 302223
- CD271 (tNGFR) APC Biolegend ME20.4 345108
- CD3 AlexaFluor 700 Becton-Dickson UCHT1 557943
- CD3 PE Biolegend UCHT1 300408
- CD34 PE-Cy7 Becton-Dickson 8G12 348791
- CD4 PE-Cy7 Biolegend OKT4 317414
- CD4 FITC Biolegend SK3 344604
- CD4 PerCP Tonbo SK3 67-0047-T500
- CD56 PerCP Biolegend HCD56 318342
- CD8 APC Tonbo OKT8 20-0086-T100
- CD8 PE-Cy7 Becton-Dickson SK1 335787
- TCR- 1G4 PE Immudex HLA-A*0201/SLLMWITQV WB3247-PE @ 1:50
- TCR-gd PE-Cy7 Biolegend B1 331221
- TCR- $\alpha\beta$ BV-421 Biolegend IP26 306722

All antibodies used at 1:200 dilution unless noted above

Validation

Antibody validations were performed by antibody suppliers per quality assurance literature provided by each supplier.

Eukaryotic cell lines

Policy information about [cell lines](#)

Cell line source(s)	The human pluripotent stem cell line MSC-iPS1 was obtained from the Boston Children's Hospital Human Embryonic Stem Cell Core (hESC).
Authentication	MSC-iPS1 was obtained from the Boston Children's Hospital Human Embryonic Stem Cell Core and verified by immunohistochemistry for pluripotency markers, teratoma formation and karyotyping.
Mycoplasma contamination	All cell lines (MSC-iPS1 cells) were tested for mycoplasma contamination.
Commonly misidentified lines (See ICLAC register)	No commonly misidentified lines were used.

Palaeontology

Specimen provenance	<i>Provide provenance information for specimens and describe permits that were obtained for the work (including the name of the issuing authority, the date of issue, and any identifying information).</i>
Specimen deposition	<i>Indicate where the specimens have been deposited to permit free access by other researchers.</i>
Dating methods	<i>If new dates are provided, describe how they were obtained (e.g. collection, storage, sample pretreatment and measurement), where they were obtained (i.e. lab name), the calibration program and the protocol for quality assurance OR state that no new dates are provided.</i>

Tick this box to confirm that the raw and calibrated dates are available in the paper or in Supplementary Information.

Animals and other organisms

Policy information about [studies involving animals; ARRIVE guidelines](#) recommended for reporting animal research

Laboratory animals	<i>For laboratory animals, report species, strain, sex and age OR state that the study did not involve laboratory animals.</i>
Wild animals	<i>Provide details on animals observed in or captured in the field; report species, sex and age where possible. Describe how animals were caught and transported and what happened to captive animals after the study (if killed, explain why and describe method; if released, say where and when) OR state that the study did not involve wild animals.</i>
Field-collected samples	<i>For laboratory work with field-collected samples, describe all relevant parameters such as housing, maintenance, temperature, photoperiod and end-of-experiment protocol OR state that the study did not involve samples collected from the field.</i>
Ethics oversight	<i>Identify the organization(s) that approved or provided guidance on the study protocol, OR state that no ethical approval or guidance was required and explain why not.</i>

Note that full information on the approval of the study protocol must also be provided in the manuscript.

Human research participants

Policy information about [studies involving human research participants](#)

Population characteristics	Healthy human blood donors were male or female and between the ages of 21 and 50.
Recruitment	Fresh blood was taken from healthy human donors recruited by fliers posted at and nearby the UCSF campus, which might incur a self-selection bias but donor cells are used anonymously so unlikely to affect results. Cells were also obtained from leukoreduction chamber residuals after Trima Apheresis from healthy human donors recruited for donation of standard blood products (Vitalant, formerly Blood Centers of the Pacific).
Ethics oversight	Studies were conducted under protocols approved by the UCSF IRB or Vitalant IRB.

Note that full information on the approval of the study protocol must also be provided in the manuscript.

Clinical data

Policy information about [clinical studies](#)

All manuscripts should comply with the ICMJE [guidelines for publication of clinical research](#) and a completed [CONSORT checklist](#) must be included with all submissions.

Clinical trial registration	<i>Provide the trial registration number from ClinicalTrials.gov or an equivalent agency.</i>
-----------------------------	---

Study protocol	Note where the full trial protocol can be accessed OR if not available, explain why.
Data collection	Describe the settings and locales of data collection, noting the time periods of recruitment and data collection.
Outcomes	Describe how you pre-defined primary and secondary outcome measures and how you assessed these measures.

ChIP-seq

Data deposition

- Confirm that both raw and final processed data have been deposited in a public database such as [GEO](#).
- Confirm that you have deposited or provided access to graph files (e.g. BED files) for the called peaks.

Data access links

May remain private before publication.

For "Initial submission" or "Revised version" documents, provide reviewer access links. For your "Final submission" document, provide a link to the deposited data.

Files in database submission

Provide a list of all files available in the database submission.

Genome browser session (e.g. [UCSC](#))

Provide a link to an anonymized genome browser session for "Initial submission" and "Revised version" documents only, to enable peer review. Write "no longer applicable" for "Final submission" documents.

Methodology

Replicates

Describe the experimental replicates, specifying number, type and replicate agreement.

Sequencing depth

Describe the sequencing depth for each experiment, providing the total number of reads, uniquely mapped reads, length of reads and whether they were paired- or single-end.

Antibodies

Describe the antibodies used for the ChIP-seq experiments; as applicable, provide supplier name, catalog number, clone name, and lot number.

Peak calling parameters

Specify the command line program and parameters used for read mapping and peak calling, including the ChIP, control and index files used.

Data quality

Describe the methods used to ensure data quality in full detail, including how many peaks are at FDR 5% and above 5-fold enrichment.

Software

Describe the software used to collect and analyze the ChIP-seq data. For custom code that has been deposited into a community repository, provide accession details.

Flow Cytometry

Plots

Confirm that:

- The axis labels state the marker and fluorochrome used (e.g. CD4-FITC).
- The axis scales are clearly visible. Include numbers along axes only for bottom left plot of group (a 'group' is an analysis of identical markers).
- All plots are contour plots with outliers or pseudocolor plots.
- A numerical value for number of cells or percentage (with statistics) is provided.

Methodology

Sample preparation

Surface staining for flow cytometry was performed by pelleting cells and re-suspending in 25-50 µL of FACS Buffer (2% FBS in PBS) plus relevant antibodies (Supplementary Table 3) for 20 minutes at 4°C in the dark. Cells were washed once in FACS buffer before resuspension for analysis

Instrument

Flow cytometric analysis was performed on an Attune NxT Acoustic Focusing Cytometer (ThermoFisher)

Software

FlowJo v.10 was used for flow cytometry data analysis.

Cell population abundance

N/A

Gating strategy

A lymphocyte gate was defined first from FSC-A v SSC-A. Singlet gates were then defined on FSC-H v FSC-W and SSC-H v SSC-W. Next, a live cell gate was defined with a Cell Viability Dye. Additional gating for cell-specific marker expression was performed if necessary, then fluorescent protein or surface gene expression was gated as shown in figure 3c or data legends for individual experiments.

Tick this box to confirm that a figure exemplifying the gating strategy is provided in the Supplementary Information.

Magnetic resonance imaging

Experimental design

Design type

Indicate task or resting state; event-related or block design.

Design specifications

Specify the number of blocks, trials or experimental units per session and/or subject, and specify the length of each trial or block (if trials are blocked) and interval between trials.

Behavioral performance measures

State number and/or type of variables recorded (e.g. correct button press, response time) and what statistics were used to establish that the subjects were performing the task as expected (e.g. mean, range, and/or standard deviation across subjects).

Acquisition

Imaging type(s)

Specify: functional, structural, diffusion, perfusion.

Field strength

Specify in Tesla

Sequence & imaging parameters

Specify the pulse sequence type (gradient echo, spin echo, etc.), imaging type (EPI, spiral, etc.), field of view, matrix size, slice thickness, orientation and TE/TR/flip angle.

Area of acquisition

State whether a whole brain scan was used OR define the area of acquisition, describing how the region was determined.

Diffusion MRI

Used

Not used

Preprocessing

Preprocessing software

Provide detail on software version and revision number and on specific parameters (model/functions, brain extraction, segmentation, smoothing kernel size, etc.).

Normalization

If data were normalized/standardized, describe the approach(es): specify linear or non-linear and define image types used for transformation OR indicate that data were not normalized and explain rationale for lack of normalization.

Normalization template

Describe the template used for normalization/transformation, specifying subject space or group standardized space (e.g. original Talairach, MNI305, ICBM152) OR indicate that the data were not normalized.

Noise and artifact removal

Describe your procedure(s) for artifact and structured noise removal, specifying motion parameters, tissue signals and physiological signals (heart rate, respiration).

Volume censoring

Define your software and/or method and criteria for volume censoring, and state the extent of such censoring.

Statistical modeling & inference

Model type and settings

Specify type (mass univariate, multivariate, RSA, predictive, etc.) and describe essential details of the model at the first and second levels (e.g. fixed, random or mixed effects; drift or auto-correlation).

Effect(s) tested

Define precise effect in terms of the task or stimulus conditions instead of psychological concepts and indicate whether ANOVA or factorial designs were used.

Specify type of analysis:

Whole brain ROI-based Both

**Statistic type for inference
(See [Eklund et al. 2016](#))**

Specify voxel-wise or cluster-wise and report all relevant parameters for cluster-wise methods.

Correction

Describe the type of correction and how it is obtained for multiple comparisons (e.g. FWE, FDR, permutation or Monte Carlo).

Models & analysis

n/a Involved in the study

- Functional and/or effective connectivity
- Graph analysis
- Multivariate modeling or predictive analysis

Functional and/or effective connectivity

Report the measures of dependence used and the model details (e.g. Pearson correlation, partial correlation, mutual information).

Graph analysis

Report the dependent variable and connectivity measure, specifying weighted graph or binarized graph, subject- or group-level, and the global and/or node summaries used (e.g. clustering coefficient, efficiency, etc.).

Multivariate modeling and predictive analysis

Specify independent variables, features extraction and dimension reduction, model, training and evaluation metrics.